WIRELESS COMMUNICATIONS AND MOBILE COMPUTING
Wirel. Commun. Mob. Comput. (2016)
Published online in Wiley Online Library (wileyonlinelibrary.com). DOI: 10.1002/wcm.2666

RESEARCH ARTICLE

Routing design avoiding energy holes in underwater acoustic sensor networks

Chaima Zidi[1,2*], Fatma Bouabdallah[2] and Raouf Boutaba[3]

[1] LIPADE Laboratory, University of Paris Descartes, Paris,France
[2] Faculty of Computing and Information Technology, King Abdulaziz University, Jeddah, Saudi Arabia
[3] School of Computer Science, University of Waterloo, Waterloo, Canada

ABSTRACT

Interest in underwater acoustic sensor networks (UW-ASNs) has rapidly increased with the desire to control the large portion of the world covered by oceans. Energy efficiency is one of the major concerns in UW-ASNs due to the limited energy budget of the underwater sensor nodes. In this paper, we tackle the problem of energy holes in UW-ASNs while taking into consideration the unique characteristics of the underwater channel. We prove that we can evenly distribute the transmission load among sensor nodes provided that sensors adjust their communication range when they send or forward the periodically generated data. In particular, we propose a balanced routing strategy along with the associated deployment pattern that meticulously determines the load weight for each possible next hop that leads to fair energy consumption among all underwater sensors. Consequently, the energy holes problem is overcome, and hence, the network lifetime is improved. To the best of our knowledge, this is the first work that addresses the energy hole problem in UW-ASNs.
Copyright © 2016 John Wiley & Sons, Ltd.

KEYWORDS

underwater acoustic sensor networks; routing; load balance; performance analysis; energy conservation

***Correspondence**

Chaima Zidi, Faculty of Computing and Information Technology, Information Technology Department, King Abdulaziz University, P.O. Box 42808, Jeddah 21551, Saudi Arabia.
E-mail: czidi@kau.edu.sa

1. INTRODUCTION

Underwater acoustic sensor networks (UW-ASNs) are considered to be a key asset in offshore exploration, tsunami warning, and mine reconnaissance [1]. Consequently, UW-ASNs are gaining a remarkable momentum in the research community. Acoustic communication is deemed to be the enabling technology for underwater networks. Indeed, electromagnetic waves tend to scatter and to be absorbed in conductive salty water within a very short distance from the transmitter. Optical waves require the transmitter and receiver to be aligned in order to form a link and tend to be effective on very short range compared with the desired communication distances.

Conceiving network protocols especially tailored for underwater acoustic networks faces serious challenges. Indeed, underwater channel imposes unique and harsh characteristics such as the high-attenuation, bandwidth-limited underwater acoustic channel and limited battery power. In fact, battery budget of underwater sensors is not only limited but most importantly cannot be recharged, as solar energy cannot be exploited. Note that, acoustic underwater communications consume larger amount of power compared with the terrestrial radio ones. Indeed, underwater communication is subject to transmission over higher distances. Moreover, more complex signal processing techniques are required at the receiver to compensate the impairments of the underwater channel.

Because of the aforementioned reasons, UW-ASNs require protocols that make judicious use of the limited energy capacity of the underwater sensor nodes. To this end, one of the major characteristics of UW-ASNs that should be appropriately exploited in order to enhance the network performance such as energy expenditure and transmission delay is manual deployment. Underwater sensors are manually bottom anchored meaning that a prior knowledge of their locations can be acquired upon deployment, especially if we deal with static underwater sensor networks. More specifically, we can take advantage of such feature in order to achieve a dedicated well-studied deployment that satisfies our application requirements especially in terms of energy conservation.

Copyright © 2016 John Wiley & Sons, Ltd.

Once the appropriate deployment is defined, another crucial way that should be well exploited to extend the lifespan of a UW-ASN is load balancing. Accordingly, all the sensors consume their energy budget as smoothly and uniformly as possible. In terrestrial wireless sensor networks (WSNs), it was shown that the closest sensors to the sink tend to deplete their provided amount of energy faster than other sensors [2–6]. This unbalanced energy consumption is liable to drastically reduce the lifetime of sensor networks; that is why it should be avoided to the largest possible extent. In fact, authors in [6] plead that by the time the nearest sensors to the sink drain their initially provided energy, sensors more distant still have up to 93% of their energy budget. Indeed, sensors in the vicinity of a static sink act as the traffic hot spots because they have significant packet load to relay. Those sensors that are 1-hop away from a static sink would suffer from a severe exhaustion of their battery power, which may cause energy holes resulting in possible network disconnection and consequently preventing reports from reaching the sink.

In this paper, a balanced routing design for avoiding energy holes in UW-ASNs is proposed and thoroughly evaluated. Our ultimate aim is to balance the energy consumption among all underwater sensors that are manually deployed according to a defined deployment pattern. Our balanced routing solution dictates that each underwater sensor can tune its transmission range among two possible levels. Each transmission range allows the sensor to reach a specified next hop. We strive for deriving the optimal load weight for each possible range that leads to fair energy consumption among all sensors in the network and hence avoiding the sink hole problem. Our proposed routing scheme is especially tailored for the underwater environment. Indeed, our routing solution takes into consideration the unique characteristics of the underwater channel such as attenuation, noise, and the dependence of usable bandwidth and transmit power on distance. In fact, once we determine the appropriate load weight for each possible transmission range, the media access control layer then adapts specific parameters, such as bandwidth and transmission power, according to the chosen transmission distance. To the best of our knowledge, this is the first work that addresses the energy sink hole problem in UW-ASNs.

Our contributions can be summarized as follows. First, we propose a well-designed deployment pattern for UW-ASN aimed at minimizing the energy consumption. Second, based on the proposed deployment, we prove that we can evenly distribute the transmission load among underwater sensors with constant data reporting provided that sensors adjust their communication ranges when they send or forward sensed data. In particular, we assume that each sensor can adjust its transmission range among two possible levels. Consequently, at the routing layer, we determine the set of possible next hops with the associated load weight that lead to a fair energy depletion among all sensors in the network. Finally, we prove that our balanced routing design outperforms the nominal communication range-based data forwarding [7] in terms of energy conservation and hence the network lifetime.

This paper is organized as follows. Section 2 presents the state of the art related to the focus of this paper. Section 3 presents a basic review of the underwater channel and introduces our network and energy model. In Section 4, we analytically formulate and solve the energy balancing problem that leads to an even energy depletion among all sensors. Results are provided in Section 5, where we compare the performance of our proposal with the nominal transmission range-based data forwarding scheme. Finally, we conclude this paper with a summary of our contributions.

2. RELATED WORK

In the past decade, underwater acoustic networks have attracted a lot of interest in the research community. While some of the already proposed solutions for WSNs may be reused, the unique characteristics of the underwater channel usually necessitate the proposal of dedicated solutions. Extensive work has been conducted up to date at different layers of the classical protocol suite. Authors in [8] provide a thorough overview of existing networking protocols for underwater networks. In this section, we mainly focus on the work related to routing in UW-ASNs and energy sink hole problem in terrestrial sensor networks.

From a routing point of view, geographical routing protocols seem appropriate for the underwater environment, where manually anchored nodes have knowledge of their coordinates at deployment time, and mobile nodes (such as autonomous underwater vehicles) have local navigation systems. Several geographical routing protocols, especially devised for underwater channel have been proposed. In [9], the design of minimum energy routing protocols especially designed for underwater environment is evaluated. Indeed, as a main contribution, authors in [9] prove that, depending on the modem performance, in dense networks there is an optimal number of hops beyond which the system performance, especially in terms of energy consumption, does not improve. In [10], two distributed routing strategies are proposed for delay-insensitive and delay-sensitive applications. In [11], a new geographical routing strategy for underwater acoustic networks is introduced and joined with power control. The main contribution of this routing scheme called FBR (Focused Beam Routing) is to dynamically establish routes on demand without damaging the network performance. In [12], the authors are mainly interested in providing a reliable routing solution especially dedicated for time-critical applications in underwater acoustic networks. To this end, they propose a multipath routing scheme based on continuous power control aimed at minimizing the energy consumption without compromising the end-to-end delay. While providing a major improvement in terms of data reliability and error recovery, crucial issue such as energy consumption during reception of a packet was not taken into account in this analysis. In [13], a mathematical framework for cross-layer optimization is stated along with

an associated protocol. Based on the unique properties of underwater environment, the proposed solution provides a joint optimization among different layers. Indeed, the proposed strategy allows each underwater node to jointly select its best next relay, the optimal transmission power, and the error correction technique that minimize the energy consumption. However, the lack of an acoustic transceiver able to dynamically adapt its parameters to instantaneously fit the link conditions limits the usefulness of this approach in practice.

When it comes to energy sink hole problem, the number of dedicated works to overcome this problem in UW-ASNs seems negligible. For this reason, we devote this section to review work related to energy sink hole problem in terrestrial WSNs. Note that, the most common approach to deal with the energy holes problem is through balancing the energy consumption through the network.

The energy sink hole problem in WSNs has gained less attention in the literature. It is worth noting that this problem was originally addressed by Guo *et al*. in [14]. They proposed an energy-balanced transmission scheme that adjusts the ratio between direct transmission to the sink and next hop transmission. Accordingly, sensor nodes are deployed in a circular disk around the sink. Each node can send a percentage of data directly to the sink and the rest to the next hop. Precisely, the authors show that sensors far away from the sink should send a larger percentage of data to the next hop, while sensors near the sink send more data directly to the sink. In [15], the authors proposed a thorough analytical model for multipath propagation that evenly distributes the energy consumption among all sensors. Indeed, they show that sending the traffic generated by each sensor node through multiple paths instead of a single best path allows performance improvement especially in terms of energy consumption. Accordingly, they derive the set of paths to be used by each sensor node and the associated proportion of utilization that minimize the energy consumption. In [16], event-driven applications in a nonuniform sensor distribution were considered. The authors proposed a blind algorithm that overcomes the energy-balancing problem without *a priori* knowledge on the occurrences of the events. In [17], authors proved that minimizing the total amount of energy along a path is only achieved when the coronas of a circular field have the same width. Unfortunately, such configuration would inevitably lead to uneven energy depletion among sensors. Consequently, they computed the optimal widths of coronas and their optimal number in order to achieve fair energy depletion of sensors. In [18], authors revealed that up to 90% of the initially provided energy budget is unused especially in static WSN model where the sensors are uniformly distributed. For this reason, they proposed a nonuniform sensor distribution strategy and showed by simulation that it can increase the total amount of sensed data. In [19], a protocol, called variable transmission range protocol (VTRP) was proposed with the aim to overcome the energy holes problem by varying the transmission power. Indeed, VTRP proposes to dynamically adapt the transmission range such that the closest sensors to the sink are bypassed, and hence, the network lifetime is increased. While VTRP assumes that the sink is static, in [7], the proposed protocol considers sink mobility and energy heterogeneity among senor nodes in order to overcome the sink hole problem.

Different from the contributions described in this section, in this paper, we present a routing solution dedicated for a specific underwater acoustic network deployment, which overcomes the energy holes problem by balancing the energy consumption through the network. As a distinguishing feature from the aforementioned described works, in our study, each sensor node has at least two possible transmission ranges. As such, each sensor node has two possible next hops to reach the sink. Consequently, we strive for deriving the appropriate load weight for each possible next hop such that the energy depletion is balanced among all sensors in the network. We believe that the proposed balanced routing design is able to efficiently overcome the energy holes problem while still remaining practical enough for real implementation.

In our study, we opt for the pre-configured static routing instead of using the adaptive dynamic routing for three main reasons. First, in our study, the sensor nodes are not actually mobile because they are manually bottom anchored. Hence, the overall network topology is static as opposed to mobile ad hoc networks, where dynamic routing is required to adapt to the frequent topological changes. Even more, in our work, we propose a well-defined deployment pattern for the underwater sensors such that our balanced pre-configured routing solution perfectly achieves the application requirements especially in terms of energy savings.

The second reason behind using the pre-configured routing is the traffic pattern. In our study, we consider continuous-monitoring applications, where each node reports periodically its data to the sink node. The amount of information generated by each sensor node is therefore known beforehand as opposed to the event-driven applications where the generated information at each sensor node is completely unknown beforehand. Finally, performing dynamic routing is not recommended for the following third reason. As known dynamic routing induces considerable exchange of signaling messages, this routing scheme requires global and real time information about the network state to make routing decisions. In computer networks where packets are large, the small control packets may impose little overhead. However, in UW-ASNs where packet size is small, they constitute a large overhead. This can be extremely costly, as a large amount of energy has to be spent to route control packets.

In response to these challenges, we propose our pre-configured balanced routing scheme. From performance evaluation perspective, we develop a model for energy consumption that meticulously captures the impact of such pre-configured static routing on the network energy expenditure.

3. MODEL AND PROBLEM DEFINITION

3.1. Basic features of underwater propagation

3.1.1. Attenuation.

The experienced attenuation in an underwater acoustic channel over a distance d in meters for a frequency f in kilohertz can be modeled in decibels by

$$10\log_{10}\left(\frac{A(d,f)}{A_0}\right)=k10\log_{10}d+\frac{d}{10^3}10\log_{10}a(f) \quad (1)$$

where A_0 is a normalizing constant, k denotes the spreading factor, and $a(f)$ denotes the absorption coefficient. $a(f)$ is empirically derived using Thorp's formula [20] in decibels per kilometer for f in kilohertz as

$$\log_{10}a(f)=0.11\frac{f^2}{1+f^2}+44\frac{f^2}{4100+f^2}+2.75\times10^{-4}f^2+0.003 \quad (2)$$

This formula is generally applied for frequencies above a few hundred hertz. For lower frequencies, it is suggested to use the following formula:

$$10\log_{10}a(f)=0.002+0.11\frac{f^2}{1+f^2}+0.011f^2 \quad (3)$$

3.1.2. Noise.

There are four different sources of noise in the ocean: turbulence, shipping, waves, and thermal noise. The overall power spectral density of the noise in decibels re $1\,\mu Pa^2/Hz$ (i.e., the power per unit bandwidth associated with the reference sound pressure level of $1\,\mu Pa^2/Hz$) can be expressed as

$$10\log_{10}N(f)=\eta_0-18\log_{10}f \quad (4)$$

where f is in kilohertz and the constant level η_0 is adjusted in accordance with a specific deployment site.

3.1.3. The signal-to-noise ratio.

The narrow band signal-to-noise ratio (SNR) is given by [21]

$$SNR(d,f)=\frac{\frac{S(f)\Delta f}{A(d,f)}}{N(f)\Delta f}=\frac{S(f)}{A(d,f)N(f)} \quad (5)$$

where $S(f)$ is the power spectral density of the transmitted signal and Δf is a narrow frequency band around f.

3.1.4. Bandwidth and transmission power definitions.

The bandwidth and the associated transmission power in the underwater environment are defined in [22]. According to [22], for each transmission range d, there exists an optimal frequency $f_0(d)$ for which the narrow band SNR is maximized. Hence, a 3-dB bandwidth, $B_{3\mathrm{dB}}(d)$, was introduced and simply refers to the range of frequencies around $f_0(d)$ for which $A(d,f)N(f) < 2A(d,f_0(d))N(f_0(d))$. Using $B_{3\mathrm{dB}}(d)$ bandwidth definition, the associated transmission power in watts necessary to provide a target SNR_0 at a distance d in meters from the source is determined as

$$P_{tx}(d)=SNR_0B_{3dB}(d)\times\frac{\int_{B_{3dB}(d)}N(f)\,df}{\int_{B_{3dB}(d)}A^{-1}(d,f)\,df} \quad (6)$$

Note that the target SNR_0 at a distance d can be expressed as function of a target packet error rate PER_{tgt} as introduced in [9]. Accordingly, by assuming the use of binary phase-shift keying, the target SNR_0 for a packet of length P_l bits can be expressed as follows:

$$SNR_0=\frac{1}{\delta}\left(\mathrm{erfc}^{-1}\left(2-2\left(1-PER_{tgt}\right)^{\frac{1}{P_l}}\right)\right)^2 \quad (7)$$

where δ is a penalty factor that accounts for signal processing inefficiencies at the receiver. Consequently, the electrical power needed to cover a distance d is given by

$$10\log_{10}P_T(d)=10\log_{10}P_{tx}(d)-170.8-10\log_{10}\xi \quad (8)$$

where $10\log_{10}P_{tx}(d)$ is the acoustic transmission power in dB re $1\,\mu Pa^2$, 170.8 dB is the conversion factor between acoustic pressure in dB re $1\,\mu Pa$ and acoustic power in watts (W), and ξ is the transducer efficiency. Figure 1 shows the generated transmission power in Watt as function of distance where $SNR_0 = 20\,dB$, $\eta_0 = 50\,dB$ re $1\,\mu Pa^2/Hz$, $A_0 = 30\,dB$, $k = 1.5$ and $\xi = 0.8$. It is worth pointing out that the transmission power is a nonlinearly increasing function of distance.

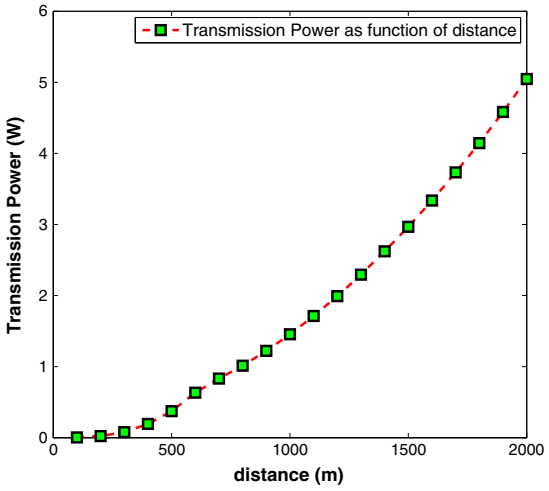

Figure 1. Transmission power as function of distance.

3.2. Energy sink hole problem

In this paper, we investigate the energy sink hole problem in UW-ASNs, where underwater sensors located close to the underwater sink are heavily used in forwarding sensed data to it. Indeed, those sensors especially the ones that are 1-hop away from the static sink act as relays to it on behalf of all other sensors, thus suffering from severe energy depletion. Extensive research efforts have been devoted to analyzing the energy sink hole problem especially in WSNs. They all agree that the energy hole problem is unavoidable in static uniformly distributed always-on WSNs where the sensors periodically report their sensed data to a static sink using their nominal communication range [14,16–18,23,24]. For this reason, most of the already undertaken research works on balancing the energy consumption focus mainly on using adjustable communication range. Indeed, by allowing each sensor to dynamically adjust its transmission range, they aim at balancing the traffic load distribution among sensors, and thus, the closest sensors to the sink are relieved of relaying task.

Our study of the energy sink hole problem in UW-ASNs is motivated by the manual deployment of underwater sensors in real world applications, and hence, efficient solutions should be provided to tackle this problem. Our goal is to balance the energy depletion of all sensors in terms of traffic forwarding (number of transmitted packets) in order to extend the network lifetime. To this end, our approach to deal with the energy sink hole problem is twofold: (i) analyzing to what extent can perfect uniform energy depletion among all sensors in the network be assured such that the energy sink hole problem in UW-ASNs is overcome and (ii) studying how can the energy sink-hole problem in manually deployed UW-ASNs be addressed. By thoroughly investigating these two issues, we aim at closely approaching the perfect uniform energy depletion among all underwater sensors in the network. To address the first issue, we conceive a data forwarding strategy for transmitting the periodically generated data from underwater source sensors to the sink. The goal of this forwarding scheme is to appropriately distribute the total data dissemination load on the individual underwater sensors such that the energy depletion is balanced among all sensors in the network. Recall that, in our study we target continuous monitoring applications, where each node reports periodically its own generated data to the sink. Consequently, we aim at distributing the total packet load (generated plus received) at each sensor among all possible next hops such that the energy consumption of each sensor is almost the same.

To address the second issue, the set of 1-hop-away neighbors of the sink should change over time, thus allowing different subsets of sensors to act as forwarders to the sink. In other words, by varying the transmission range of manually deployed sensors, the number of hops to reach the sink is continuously varying. For instance, suppose that a sensor U is $2r$ away from the sink S. If the underwater sensor U uses a transmission range of r, then U is 2-hop away from S. However, if U adopts a transmission range of $2r$ then U is 1-hop away from S. Consequently, we propose that U sends a fraction of its total load using a transmission range of r, and the remaining portion is directly sent to the sink using a transmission range of $2r$.

To recapitulate, in our work, each sensor is responsible of deriving the appropriate load weight with the associated transmission range, namely, potential next hop, that evenly distribute the energy consumption among underwater sensors. Similar objectives have been achieved in the literature by considering mobile sink [3,7]. However, in our work, we tackle the energy sink hole problem by considering a static underwater sensor deployment strategy where underwater sensors are manually placed in a circular sensor field centered at one static sink.

3.3. Network and energy model

In underwater environment, the deployment is generally sparser compared with terrestrial sensor networks because of the high cost of underwater sensors and the severe deployment challenges. Indeed, underwater sensors are manually anchored to the bottom of the ocean with deep ocean anchors. Such apparently stumbling characteristics should be appropriately exploited in order to enhance the network performance such as energy expenditure and transmission delay. Indeed, the manual and sparse deployment of UW-ASN not only highly reduces the number of deployed sensors but also allows the administrator to acquire a precise knowledge of their number in addition to their precise location that makes their precise deployment possible, which was extremely unrealistic with terrestrial sensor networks. This study is the first to exploit the sparse and manual deployment of UW-ASNs in order to propose a dedicated deployment pattern that approaches the perfect balanced energy depletion among underwater sensors.

The proposed deployment strategy considers a two-dimensional shallow underwater sensor network. A set of sensors are anchored to the ocean bottom and endowed with a floating buoy. The buoy can be inflated by a pump in order to bring the sensor towards the ocean surface. Note that, in such architecture, if we consider static underwater sensor network, the bottom mounted sensors have a complete knowledge of their geographical position upon deployment. In order to approach the perfect uniform energy depletion, sensors are placed in a circular sensor field of radius R centered at the sink. The sensor field is virtually partitioned into disjoint concentric sets termed coronas of constant width r. The width of each corona is at most $d_{tx-\max}$, the maximum transmission range of an underwater acoustic sensor. Consider K to be the number of coronas around the sink.

$$K = \left\lfloor \frac{R}{r} \right\rfloor \tag{9}$$

For example, in Figure 2, $K = 5$; hence, the sensor field is partitioned into five coronas B_1, B_2, B_3, B_4, and B_5.

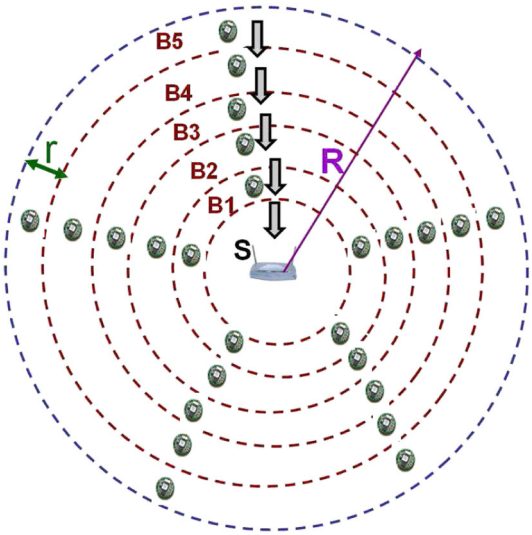

Figure 2. Underwater acoustic sensor network model.

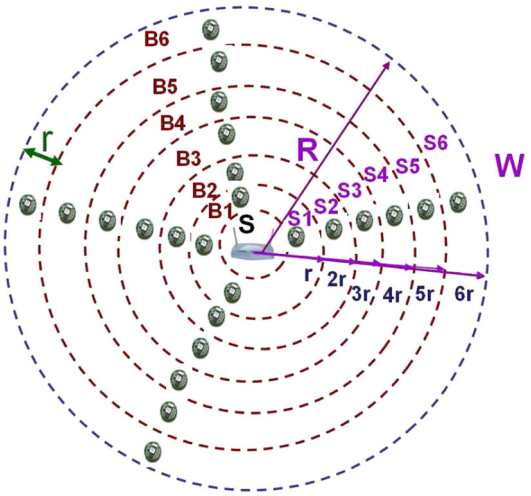

Figure 3. A wedge W and the associated sectors.

In the remainder of this paper, we consider a continuous reporting sensor application where the average number of reports generated per unit of time by each sensor node is denoted by A. Moreover, we assume that the energy consumption of sensors is due to data reception and transmission. In fact, because in underwater environment, the deployment is generally sparse, the energy depletion due to overhearing can be neglected. More precisely, the energy spent in transmitting one packet of length P_l bits over a distance d is given by

$$E_{tx}(d) = P_T(d) \times T_{tx}(d) \tag{10}$$

where $T_{tx}(d)$ is the transmission time given by

$$T_{tx}(d) = \frac{P_l}{C_{3dB}(d)} \tag{11}$$

where $C_{3dB}(d)$ is the maximum allowed capacity over $B_{3\mathrm{dB}}(d)$. According to [21],

$$C_{3dB}(d) = \int_{B_{3\mathrm{dB}}(d)} \log_2\left(1 + \frac{P_{tx}(d)/B_{3\mathrm{dB}}(d)}{A(d,f)\,N(f)}\right) df \tag{12}$$

Likewise, the energy spent in receiving one P_l bits packet is given by

$$E_{rx}(d) = P_{rx}^0 \times T_{tx}(d) \tag{13}$$

where P_{rx}^0 is the electronics power.

According to the dedicated deployment pattern discussed earlier, routing is relatively straightforward. Each packet is forwarded from the source to the sink by crossing adjacent coronas through the immediately adjacent sensors. Figure 2 illustrates a possible path along which a packet from one sensor in the outermost corona is routed to the sink. Notice that, in this example, each hop involves the immediately adjacent neighbor from adjacent corona. More precisely, our sensor field can be seen as a set of wedges. Each wedge W is virtually partitioned into K sectors, $S_1, S_2, \ldots, S_K$ by its intersection with K concentric circles, centered at the sink, and of monotonically increasing radius $r, 2r, 3r, \ldots, Kr$, as shown in Figure 3. Each sector contains exactly one sensor that has to forward the cumulative traffic coming from its predecessors to one of its possible successors. Specifically, in our study, we assume that each sensor is capable of adjusting its transmission range in order to send the appropriate fractions of packet load to the adjacent successor and the one after. More details are given in the next section.

4. BALANCING ENERGY EXPENDITURE

In this paper, we strive for efficiently routing the reports to the sink node by balancing the energy consumption throughout the network. By doing so, we aim at improving the UW-ASNs lifetime. In our study, all the sensor nodes transmit periodically their reports to the sink node, denoted by $\mathcal{S}$. We target here continuous-monitoring applications, one of the most important classes of UW-ASN applications. The average number of reports generated per unit of time by each sensor node is denoted by A. In this section, we turn to the task of evaluating the energy expenditure per sensor in an arbitrary corona B_i with $i \geq 1$. Observe that, according to our routing strategy, every node in a given wedge W and a generic corona B_i, $(1 \leq i \leq K)$, is called upon to serve two kinds of paths:

- Paths originating at an underwater sensor located in the same wedge W but in a different corona B_j with $i < j \leq K$, and
- Paths emanating from the same sensor in B_i.

It is easy to show that the total number of paths that may involve a specific node in a given wedge W and in corona B_i includes all possible paths in W except those originating in one of the coronas $B_1, B_2, \ldots$ and B_{i-1}.

In this paper, we approach the efficient routing of reports to the sink node by appropriately distributing the total data dissemination load on the individual underwater sensors such that a fair energy depletion is assured among all sensors in the network, and hence, the UW-ASN lifetime is enhanced.

In this study, we suppose that for each sensor node located at corona B_i in a specific wedge W, the next hop to send generated reports to the sink $\mathcal{S}$ can be the sensor located in B_{i-1} or B_{i-2} in the same wedge W. In other words, we suppose that

$$d_{tx-\max} \in \{r,\ 2r\} \tag{14}$$

Considering a wedge W, we associate to each possible next hop located in B_{i-1}or B_{i-2} a respective weight $\beta_1^i$and β_2^i such that $\beta_1^i + \beta_2^i = 1,\ \forall i,\ 1 \leq i \leq K$. Consequently, the total number of packets per unit of time, A_i, handled by sensor in corona B_i and wedge W, can simply be expressed as follows:

$$A_i = A + \beta_1^{i+1} A_{i+1} + \beta_2^{i+2} A_{i+2} \tag{15}$$

where $\beta_j^{i+j} = 0$ for $j = 1, 2$, if $i + j > K$.

Consequently, the average transmission energy, E_{tx}^i, consumed by a sensor in corona B_i and wedge W can be derived as follows:

$$E_{TX}^i = \beta_1^i A_i E_{tx}(r) + \beta_2^i A_i E_{tx}(2r) \tag{16}$$

where $\beta_j^i = 0$ for $j = 1, 2$ if $i - j < 0$.

Likewise, the average reception energy, E_{rx}^i, consumed by a sensor in corona B_i and wedge W can be expressed as follows:

$$E_{RX}^i = \beta_1^{i+1} A_{i+1} E_{rx}(r) + \beta_2^{i+2} A_{i+2} E_{rx}(2r) \tag{17}$$

where $\beta_j^{i+j} = 0$ for $j = 1, 2$ if $i + j > K$.

Finally, the total energy consumed by a sensor in corona B_i and wedge W is

$$E^i = E_{TX}^i + E_{RX}^i \tag{18}$$

Recall that the goal of our work is to tailor the coronas in such way that the energy expenditure is balanced across all the coronas. Consequently, our problem can be stated as follows:

$$\begin{aligned} &\text{Given } K,\ r,\ d_{tx-\max} \\ &\text{Find } \beta_1^i, \beta_2^i \forall i, 1 \leq i \leq K \\ &\text{such that } E^1 = E^2 = \ldots = E^K \\ &\text{subject to} \\ &\beta_1^i + \beta_2^i = 1, \forall i, 1 \leq i \leq K \end{aligned} \tag{19}$$

In the next section, we strive for approaching the perfect uniform energy depletion by determining, for each sensor node, the next possible hops with the associated load weight that better approach the balanced energy expenditure among underwater sensors. Note that, in practical applications, a centralized computing center will be in charge of making the network planning by providing every sensor with the appropriate sending weights to every possible upstream sensor on the way to reach the sink. In what follows, we denote $E_{rx}(jr)$ as E_{rx}^j, $E_{tx}(jr)$ as E_{tx}^j, and the vector $\beta^i = \left(\beta_l^i\right)_{1 \leq l \leq 2}$.

4.1. Iterative process

The first analytical approach of the perfect uniform energy depletion is using an iterative process. As it turns out, the β^is can be determined iteratively in a natural way. In the first iteration, we suppose that we only have the corona B_1 of width r. In this case, the total traffic of each sensor in B_1 is exclusively composed of the locally generated traffic A and clearly β_1^1 equal to 1. In the second iteration, we add corona B_2, and knowing β_1^1, we try to balance the energy expenditure between B_1 and B_2 by determining β_1^2 and β_2^2. More precisely, by adding B_2, the total traffic of B_1 increases as there is a newly received traffic from B_2. Consequently, our previously established balance is perturbed. To re-arrange such imbalance, we compute β_1^2 and β_2^2. Note that β_2^2 denotes the traffic weight that has to be sent directly from sensor in B_2 to the sink.

Generally speaking, suppose that we reach iteration j, and hence, the energy consumption between j coronas is balanced. Adding corona B_{j+1} will disturb the previously established balance as the total traffic in each corona will inevitably increase. Knowing $\beta^1, \beta^2, \ldots, \beta^j$, we settle once again our balance by determining β^{j+1}. Note that for the newly added corona B_{j+1}, $A_{j+1} = A$, and $E_{RX}^{j+1} = 0$.

As we shall see shortly, β^2 is obtained after adding corona B_2 and as a result of writing $E^2 = E^1$. By the same way, after adding corona B_3, β^3 is obtained from $E^3 = E^2$ and $E^3 = E^1$. More generally, at iteration $j + 1$, β^{j+1} is obtained from $E^{j+1} = E^j = \ldots = E^1$. The iterative process is straightforward; the details are presented next.

4.1.1. Calculation of the cumulative traffic.

Let us start by iteratively expressing the cumulative traffic. For this purpose, at each iteration $j + 1$, we newly derive $A_{j-k}; \forall\ 0 \leq k \leq j - 1$.

$$\begin{aligned}
&\forall\ 1 \le j+1 \le K\ ; A_{j+1} = A\\
&\forall\ 0 \le k \le j-1\ ;\\
&A_{j-k} = \left[\alpha_{0k} + \alpha_{1k}\beta_1^{j+1} + \alpha_{2k}\beta_2^{j+1}\right] \times A
\end{aligned}$$

where

$$\begin{aligned}
\beta_2^{j+1} &= 0 \qquad \text{if } k = j-1\\
\alpha_{00} &= 1;\ \alpha_{0(-1)} = 1\\
\alpha_{0k} &= 1 + \alpha_{0(k-1)}\beta_1^{j-(k-1)} + \alpha_{0(k-2)}\beta_2^{j-(k-2)}\\
\alpha_{1(-1)} &= 0;\ \alpha_{2(-1)} = 0; \alpha_{21} = 1; \alpha_{10} = 1; \alpha_{20} = 0;\\
\alpha_{1k} &= \alpha_{1(k-1)}\beta_1^{j-(k-1)} + \alpha_{1(k-2)}\beta_2^{j-(k-2)}\\
\alpha_{2k} &= \alpha_{2(k-1)}\beta_1^{j-(k-1)} + \alpha_{2(k-2)}\beta_2^{j-(k-2)}
\end{aligned} \tag{20}$$

(proof in the Appendix).

4.1.2. Calculation of energy consumption in transmission and reception.

Recall that our objective is to determine β^{j+1}, for each iteration $j+1$, which balances the energy consumption between $B_1, B_2, \ldots, B_{j+1}$. Consequently, at each iteration $j+1$, we strive for deriving the unknown vector β^{j+1} of size 2. For this purpose, we aim at expressing E_{TX}^{j+1}, E_{TX}^{i}, and E_{RX}^{i} ($\forall\ 1 \le i < j+1$) as function of β^{j+1}. Consequently, by writing $E_{TX}^{j+1} = E^j = \ldots = E^1$, we obtain a system of $j+1$ equations with two unknowns. Let us start by expressing the straightforward E_{RX}^{j+1} and E_{TX}^{j+1}.

$$\begin{aligned}
&\forall 1 \le j+1 \le K\\
&E_{RX}^{j+1} = 0\\
&E_{TX}^{j+1} = \left[AE_{tx}^1\beta_1^{j+1} + AE_{tx}^2\beta_2^{j+1}\right]\\
&\qquad = TX_1^{j+1}\beta_1^{j+1} + TX_2^{j+1}\beta_2^{j+1}
\end{aligned} \tag{21}$$

where $TX_l^{j+1} = AE_{tx}^l$ for $l = 1, 2$.

Note that our ultimate goal is to express our problem as a system of linear equations, at each iteration. We succeed to linearly express E_{TX}^{j+1} as function of β^{j+1}. Now, let us derive E_{TX}^{i} and E_{RX}^{i} ($\forall\ 1 \le i < j+1$) as function of β^{j+1}.

$$\begin{aligned}
E_{TX}^{i} &= \left[A_i\beta_1^i E_{tx}^1 + A_i\beta_2^i E_{tx}^2\right]\\
&= A_i\left[\beta_1^i E_{tx}^1 + \beta_2^i E_{tx}^2\right] = TX_0^i + \sum_{l=1}^{2} TX_l^{j-i}\beta_l^{j+1}
\end{aligned} \tag{22}$$

where $\beta_2^{j+1} = 0$ if $j+1 = 1$ and $\beta_2^i = 0$ if $i = 1$.

Now, let us find E_{RX}^{i}, $\forall 1 \le i < j+1$

$$\begin{aligned}
E_{RX}^{i} &= \beta_1^{i+1}A_{i+1}E_{rx}^1 + \beta_2^{i+2}A_{i+2}E_{rx}^2\\
&= RX_0^i + RX_1^{j-i}\beta_1^{j+1} + RX_2^{j-i}\beta_2^{j+1}
\end{aligned} \tag{23}$$

where $\beta_2^{i+2} = 0$ if $i = j$, and if $i = j-1$, then $E_{RX}^{i} = RX_0^i + RX_1^{j-i}\beta_1^{j+1} + AE_{rx}^2\beta_2^{j+1}$.

For more details on the calculation of transmission and reception energy, we present a detailed derivation of Equations (22) and (23) in the Appendix.

4.2. Problem statement

Now that we succeed to express our problem as a system of linear equations, we finally obtain

$$\begin{aligned}
&\forall\ 1 \le j+1 \le K\\
&\forall 1 \le i < j+1\\
&E_{TX}^{j+1} = E_{TX}^{i} + E_{RX}^{i}\\
&\quad \Leftrightarrow \left(TX_1^{j+1} - TX_1^{j-i} - RX_1^{j-i}\right)\beta_1^{j+1} +\\
&\quad + \left(TX_2^{j+1} - TX_2^{j-i} - RX_2^{j-i}\right)\beta_2^{j+1} = TX_0^i\\
&\quad + RX_0^i\beta_1^{j+1} + \beta_2^{j+1} = 1
\end{aligned} \tag{24}$$

Let TX_{j+1} be a matrix of size $(j+1, 2)$ such that $TX_{j+1} = \left(TX_{i,l}\right)_{\substack{1 \le i \le j+1\\ 1 \le l \le 2}}$

$$\begin{aligned}
TX_{i,1} &= TX_1^{j+1} - TX_1^{j-i} - RX_1^{j-i};\ \forall\ 1 \le i < j+1\\
TX_{i,2} &= TX_2^{j+1} - TX_2^{j-i} - RX_2^{j-i};\ \forall\ 1 \le i < j+1\\
TX_{(j+1),1} &= 1\\
TX_{(j+1),2} &= 1
\end{aligned} \tag{25}$$

Recall that β^{j+1} is a column vector such that $\beta^{j+1} = \left(\beta_l^{j+1}\right)_{1 \le l \le 2}$ and let us define C as $\left(C_0^i\right)_{1 \le i < j+1}$ such that $C_0^i = TX_0^i + RX_0^i$; $\forall\ 1 \le i < j+1$ and $C_0^{j+1} = 1$. In this case, our system can be written as $TX_{j+1}\beta^{j+1} = C$. Note that $\beta_1^{j+1} + \beta_2^{j+1} = 1, \forall\ 1 \le j+1 \le K$.

Note that, if $j+1 = 2$, then we have a system of two equations with two unknown variables. Consequently, TX_{j+1} is a square matrix of size 2. Hence, we can easily solve $TX_{j+1}\beta^{j+1} = C$, and thus, the perfect uniform energy depletion is reached. However, if $j+1 > 2$, then our system is actually composed of $j+1$ equations $\left(E^{j+1} = E^j = ... = E^1\right)$ with only two unknown variables. Consequently, we have much more equations than needed, and hence, achieving perfect uniform energy depletion is impossible. For this reason, we slightly deviate our original goal to become that of minimizing the difference in energy consumption among different coronas. We try to numerically solve our partial uniform energy depletion problem after reformulating it as follows:

$$\begin{aligned}
&\text{Given } K,\ r,\ d_{tx-\max}\\
&\text{Find } \beta_1^{j+1},\ \beta_2^{j+1}\\
&\min_{\beta^{j+1}} \left\| TX_{j+1}\beta^{j+1} - C \right\|\\
&\text{subject to}\\
&\beta_1^{j+1} + \beta_2^{j+1} = 1\\
&\beta_1^{j+1} \ge 0 \text{ and } \beta_2^{j+1} \ge 0
\end{aligned} \tag{26}$$

This constrained nonlinear optimization problem can be easily solved using 'fmincon' function in the Matlab optimization toolbox. Note that fmincon is a powerful optimization tool that uses three well-known methods, namely, active set, trust region reflective,x and interior point.

5. PERFORMANCE EVALUATION

In this section, we present a thorough comparison study between our balanced routing solution ($d_{tx-\max} \in \{r, 2r\}$) and the nominal communication range-based data forwarding [7] (i.e., ($d_{tx-\max} = r$)). Results are derived analytically. Recall that in our model the underwater sensor nodes perform continuous monitoring of the supervised circular area of radius R. Our circular sensor field centered at the sink is partitioned into disjoint concentric coronas of fixed width r. Each underwater sensor periodically reports with rate A the locally generated data to the sink over several hops. At each hop, the traffic emanating from the local sensor must be merged with route-through traffic. Each packet is forwarded from the source to the sink by crossing coronas located in the same wedge. Power control was performed by determining the minimum power required to achieve a packet error probability of 0.04 at the receiver and a SNR penalty of $\delta = -10$ dB providing thus a target SNR_0 of 20 dB. The parameters setting in our analysis are listed in Table I.

We first analyze the results regarding our balanced routing strategy for a circular sensor field of radius $R = 1000$ m and corona width $r = 100$ m resulting in a total number of coronas equals 10. Each sensor in each corona is supposed to generate 10 packet/s. We study the impact of using variable transmission range ($d_{tx-\max} \in \{r, 2r\}$) on both packet load and energy consumption for every corona. The bandwidths and center frequencies adopted in our study configuration are reported in Table II.

First, let us discover $\beta = (\beta^i)_{1 \le i \le 10}$ matrix of our balanced routing scheme with $d_{tx-\max} \in \{r, 2r\}$. We want to point out that the β matrix is derived with the purpose of evenly distributing the energy consumption among different coronas. Table III reports the β^i vectors for each corona. Accordingly, in order to minimize the energy consumption gap between different coronas, much more packets should be sent to the 2-hop away corona. In other words, in order to balance the energy consumption among different coronas, most of the accumulated traffic should be forwarded using $d_{tx-\max} = 2r = 200$ m. Indeed, underwater sensors in the second corona should send 98% of their accumulated traffic directly to the sink. In the same way, sensors in coronas 4, 6, 7, 8, and 9 have to disseminate more than 80% of their total packet load to the 2-hop away coronas. The least percentage is achieved in the third corona. In fact, the sensor in corona 3 sends 65% of its traffic to the first band against only 35% to the second corona. As a result, it is clear enough that it is highly preferred to send packets load 2-hop away in order to balance the energy consumption.

According to Table III, the packet load distribution is shown in Figure 4. Note that adopting a nominal communication range-based data forwarding with $d_{tx-\max} = r$

Table I. Parameters setting.

Packet length P_l	1024 bits
SNR_0	20 dB
Initial energy	1 J
Data rate A	10 packet/s
P_{rx}^0	0.75 W
η_0	50 dB re 1 μ Pa^2/Hz
A_0	30 dB
Spreading factor k	1.5
Transducer efficiency ξ	0.8

Table II. Bandwidths and center frequencies.

	$d_{tx-\max} = 100$ m (kHz)	$d_{tx-\max} = 200$ m (kHz)
B_{3dB}	24.46	31.51
f_c	47.77	44.25

Table III. β matrix when $R = 1000$ m and $r = 100$ m.

	Band $(i-1)$	Band $(i-2)$
Band 1	1	0
Band 2	0.02	0.98
Band 3	0.35	0.65
Band 4	0.14	0.86
Band 5	0.25	0.75
Band 6	0.17	0.83
Band 7	0.18	0.82
Band 8	0.15	0.85
Band 9	0.13	0.87
Band 10	0.1	0.9

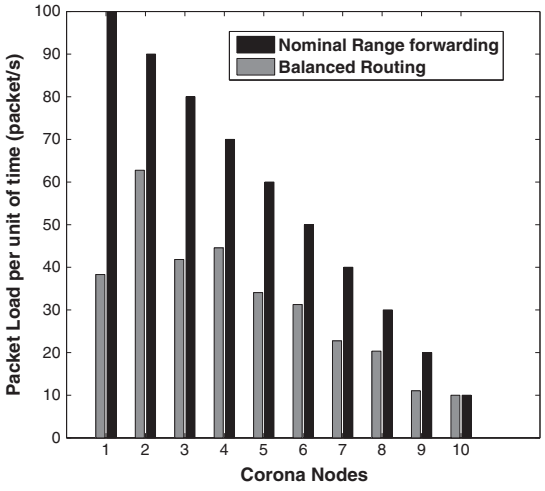

Figure 4. Packet load distribution per corona when $R = 1000$ m and $r = 100$ m.

leads to a total traffic of 100 packet/s at sensors in corona 1. This amount of accumulated traffic at corona 1 is highly decreased (less than 40 packet/s) with our balanced routing solution ($d_{tx-\max} \in \{r, 2r\}$). This gain is more importantly highlighted in Figure 5. In fact, Figure 5 shows the energy consumption for each sensor in the corresponding corona. Accordingly, a 74% of energy saving is achieved at corona 1. It is worth noting that using our balanced routing strategy leads to a maximum energy expenditure of 0.065 W at sensors in corona 2. However, according to the nominal communication range-based data forwarding, a maximum energy consumption of 0.146 W is achieved as expected at corona 1. Consequently, an energy saving of 55.5% is accomplished thanks to our balanced routing scheme. We would like to point out that the energy consumption per corona is not proportional to the packet load distribution as shown in Figures 4 and 5. Indeed, as depicted in Figure 1, the energy expenditure depends nonlinearly on the transmission distance, which justifies the non-proportionality between packet load distribution and the energy consumption. Consequently, balancing the energy consumption does not really mean balancing the packet load distribution.

Let us now evaluate the gain that can be achieved by our balanced routing solution ($d_{tx-\max} \in \{r, 2r\}$) over the nominal communication range-based data forwarding ($d_{tx-\max} = r$) for different field radius as well as different corona width. Note that this comparison study is mainly conducted in terms of energy consumption and network lifetime. From an energy depletion point of view, we consider the maximum consumed amount of energy among all coronas. When it comes to network lifespan, we define the network lifetime simply as the time for the first node in the network to drain its energy budget. In other words, the network lifetime is given by

$$T_{net\_lifetime} = \frac{E_{init}}{\max_{U \in corona\_nodes} E(U)} \quad (27)$$

where E_{init} is the initial amount of energy provided to each sensor node and U refers to an arbitrary underwater sensor in our field.

Figure 6 shows the energy expenditure as function of field radius when the corona width remains fixed and equal to $r = 100$ m. Recall that the energy value considered for each field radius is the maximum consumed energy among all coronas. As expected, as the field radius increases the energy consumption increases because the number of coronas grows. Consequently and as depicted in Figure 7, the network lifetime decreases with the increase of the field radius. Note that our balanced routing solution achieves up to 62% of energy saving for a field radius of 500 m, and a minimum energy saving of 46% is guaranteed in each configuration.

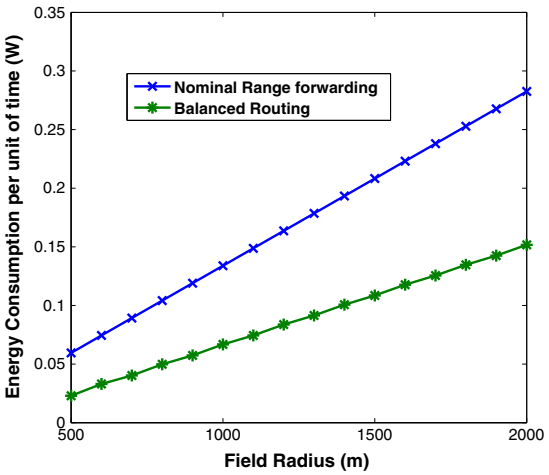

Figure 6. Energy consumption for different field radius when $r = 100$ m.

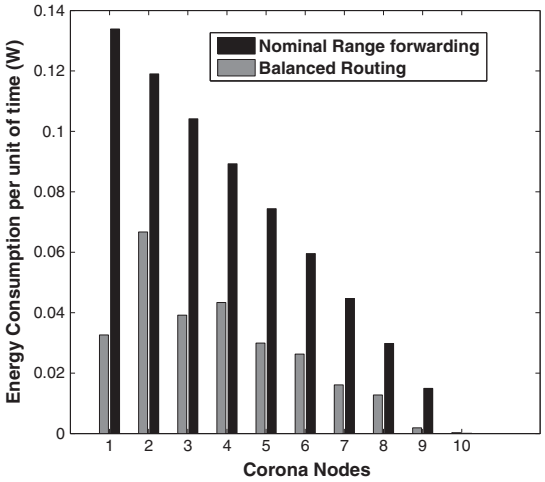

Figure 5. Energy consumption per corona when $R = 1000$ m and $r = 100$ m.

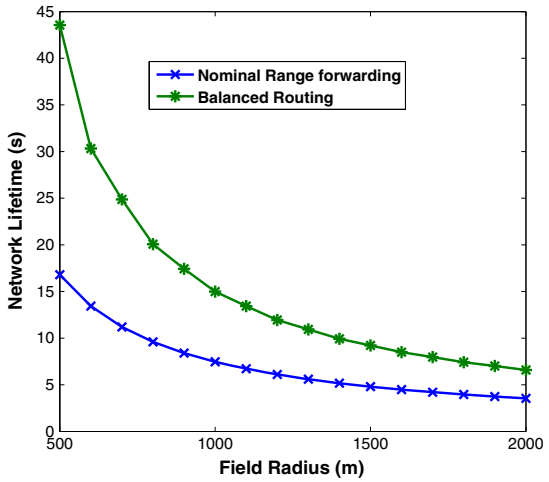

Figure 7. Network lifetime for different field radius when $r = 100$ m.

Now, let us assess the impact of varying the corona width on the system performance. To achieve this, we consider a fixed field radius of 2000 m while varying the corona width from 50 to 500 m.

The most revealing values of B_{3dB} bandwidths and center frequencies adopted for various corona widths are reported in Table IV.

Considering Figure 8, the energy expenditure decreases when the corona width increases. In fact, rising the corona width reduces the number of coronas, and consequently, the packets load is reduced. Here again, our balanced routing strategy achieves better performance than nominal communication range-based data forwarding. In fact, according to Figures 8 and 9, better energy savings and longer network lifetime are guaranteed with our balanced routing solution. Note that for high corona widths, our solution achieves slightly better energy saving than the nominal communication range-based data forwarding ($d_{tx-\max} = r$). Indeed, according to Figure 1, for high value of corona width (r), sending over a distance of $2r$ consumes much more energy than sending over a distance of r because the transmission power is a nonlinear function of distance. For this reason, we expect, for high value of r, our balanced solution converges to the nominal communication range solution.

In order to gain more insight regarding the system performance for each corona, let us closely inspect the energy consumption as well as the packet load for the

Table IV. Bandwidths and center frequencies.

	B_{3dB} (kHz)	f_c (kHz)
$r = 400$ m	43.69	38.16
$r = 500$ m	46	36.95
$r = 700$ m	41.77	32.14
$r = 900$ m	32.36	25.89
$r = 1000$ m	29.55	23.92

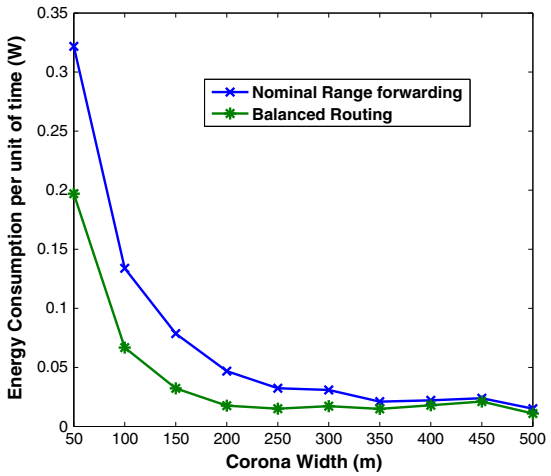

Figure 8. Energy consumption for various corona width when $R = 2000$ m.

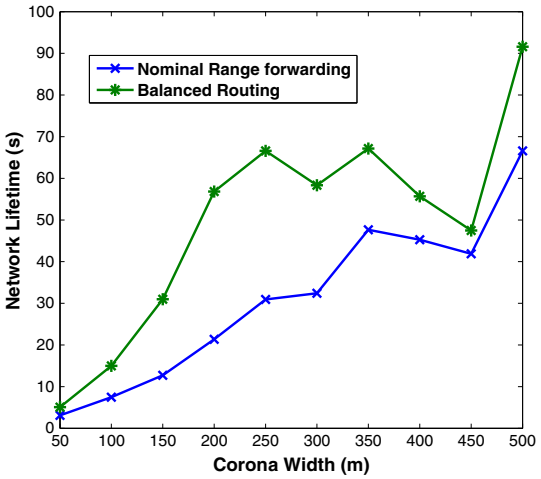

Figure 9. Network lifetime for various corona width when $R = 2000$ m.

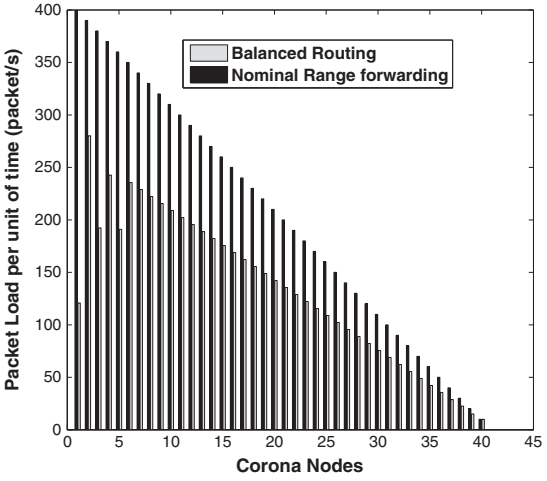

Figure 10. Packet load distribution per corona when $R = 2000$ m and $r = 50$ m.

extreme cases, namely, $R = 2000$ and $r = 50$; $R = 2000$ and $r = 250$; $R = 500$ and $r = 50$, and $R = 500$ and $r = 250$. Figures 10–17 well confirm the performance improvement gained by adopting our balanced routing strategy. It is clearly seen that, even in the extreme cases, significant energy conservation and more balanced packet load distribution are assured by balanced routing scheme ($d_{tx-\max} \in \{r, 2r\}$) over the nominal communication range-based data forwarding ($d_{tx-\max} = r$). Indeed, for a field radius of 2000 m and a corona width of 50 m, an energy conservation of 36% is achieved by our solution. Note that a perfect energy balancing is established for a field radius of 500 m and a corona width of 250 m leading to an energy conservation of 73% . Here again, we point out that a perfect balance of energy consumption as shown in Figure 17 does not mean a perfect load distribution as depicted in Figure 16 because the transmission power is a nonlinear function of transmission distance.

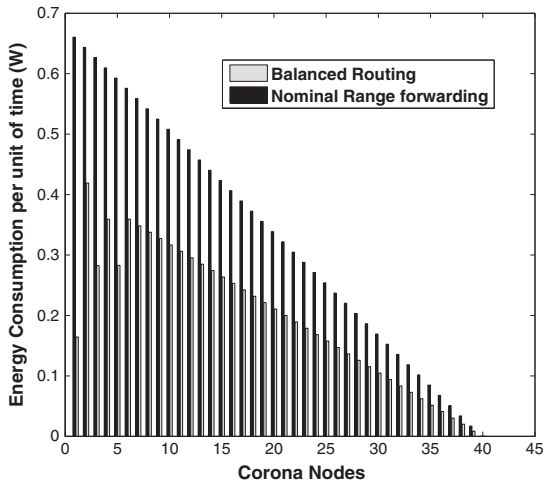

Figure 11. Energy consumption per corona when $R = 2000$ m and $r = 50$ m.

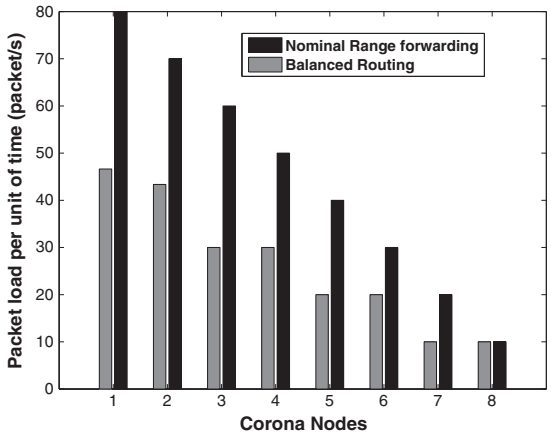

Figure 12. Packet load distribution per corona when $R = 2000$ m and $r = 250$ m.

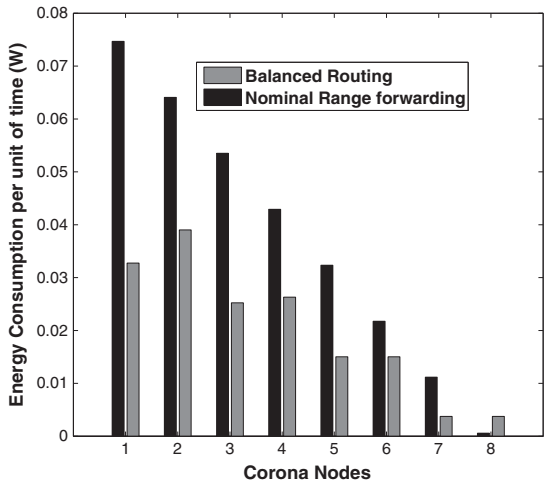

Figure 13. Energy consumption per corona when $R = 2000$ m and $r = 250$ m.

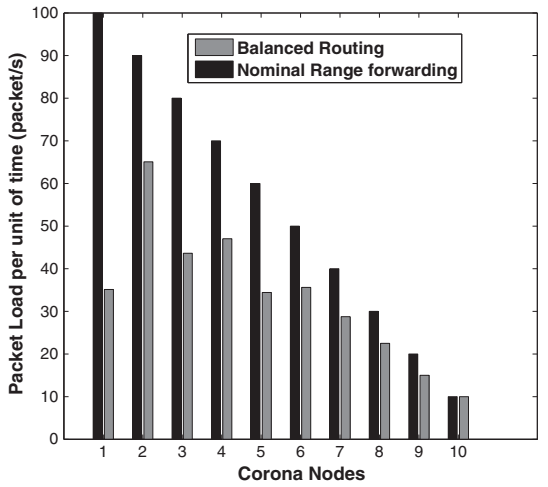

Figure 14. Packet load distribution per corona when $R = 500$ m and $r = 50$ m.

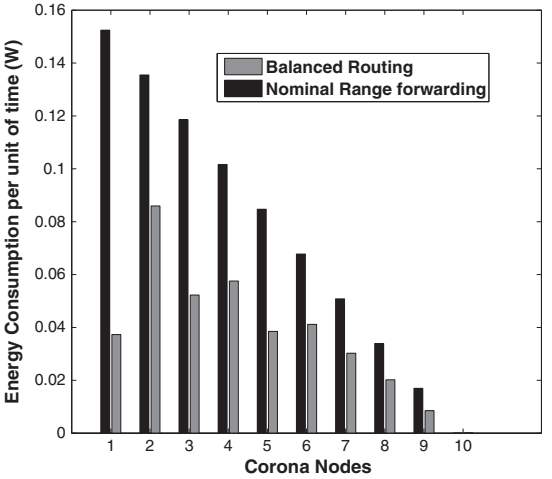

Figure 15. Energy consumption per corona when $R = 500$ m and $r = 50$ m.

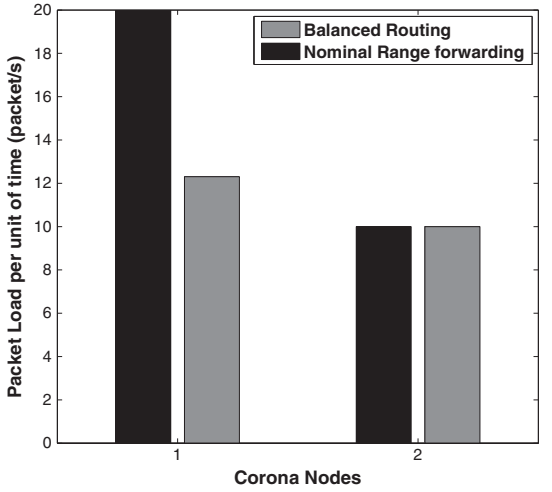

Figure 16. Packet load distribution per corona when $R = 500$ m and $r = 250$ m.

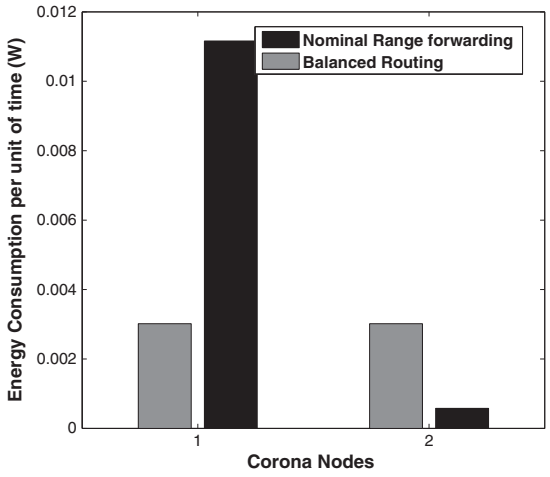

Figure 17. Energy consumption per corona when $R = 500\,\text{m}$ and $r = 250\,\text{m}$.

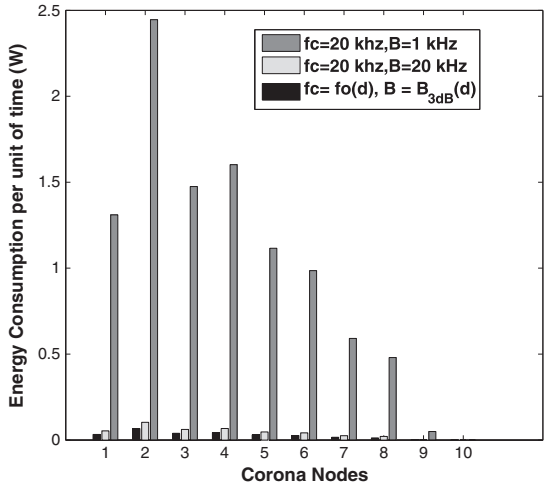

Figure 18. Energy consumption per corona for various frequency band.

Finally, to justify the use of $B_{3\text{dB}}$ bandwidth definition, let us evaluate its contribution to energy saving in our model. Recall that, according to [22], there is an optimal bandwidth and its corresponding optimal transmission frequency for each transmission distance. Consequently, for each selected transmission range, we use the $B_{3\text{dB}}(d)$ bandwidth centered on a tone of frequency $f_c = f_0(d)$. Using our balanced routing scheme with $d_{tx-\max} \in \{r, 2r\}$, Figure 18 illustrates the effect of independently changing the bandwidth and the center frequency while applying the same $\beta = (\beta^i)_{1\leq i\leq 10}$ matrix on traffic load distribution. The system performance is analyzed for two different center frequencies $f_c = 20\,\text{kHz}$ and $f_c = f_0(d)$. With $f_0(d)$, we use the $B_{3\text{dB}}(d)$ bandwidth definition. However, for $f_c = 20\,\text{kHz}$, the system performance is analyzed for two different bandwidths $B = 1\,\text{kHz}$ and $B = 20\,\text{kHz}$. When the center frequency remains fixed and equal to 20 kHz, an important energy saving is achieved when increasing the bandwidth, for each corona. In fact, with a greater bandwidth, the bit duration $1/B$ is highly reduced and thus the energy consumption. Most importantly, note that the optimal energy consumption is accomplished with $f_c = f_0(d)$ and its corresponding $B_{3\text{dB}}(d)$ bandwidth. As shown in Figure 18, sensors in corona 2 consume the maximum amount of energy, for each frequency and bandwidth allocation scheme. However, the energy expenditure of sensors in corona 2 is reduced with $f_c = f_0(d)$ and its corresponding $B_{3\text{dB}}(d)$ bandwidth. We want to point out that our routing solution tries to optimize the energy consumption by looking most importantly for the best traffic distribution among coronas and by applying the optimal frequency and bandwidth. As such, a comprehensive solution is proposed.

In order to further assess the performance of our proposed energy balancing routing scheme, let us consider a deployment pattern where the underwater sensors are non-equally spaced. In other words, let us suppose that the corona width in our sensor field is variable. Note that such study can be of great importance in order to assess the efficiency of our energy balancing routing protocol in a temporally variant channel. Indeed, in a time variant context, nodes are prone to be not equally spaced. To have an idea about the efficiency of our protocol in such condition, let us consider a deployment pattern where the corona width is following an arithmetic progression with an initial term r_0, which is the width of the first corona B_1, and a common difference c_d. More precisely, the width, r_i, of a given corona B_i is expressed as follows:

$$r_i = r_0 + (i-1)\,c_d \tag{28}$$

It is worth pointing out that if $r_i > d_{tx-\max}$, then r_i will be limited to only $d_{tx-\max}$. In other words, once r_i exceeds $d_{tx-\max}$, the remaining field radius will be portioned into coronas of fixed size $d_{tx-\max}$ where the lat corona can be of width less than $d_{tx-\max}$.

In this study, we consider a sensor field of radius $R = 2000\,\text{m}$, where the first corona is of width $r_0 = 50\,\text{m}$ with a common difference $c_d = 50\,\text{m}$ and $d_{tx-\max} = 400\,\text{m}$. In this case, our sensor field is partitioned into nine coronas such that the first one is of width 50 m and the subsequent ones, up to the eighth corona, are following an arithmetic progression with a difference 50 m. The last corona is of width 200 m because the field radius is limited to 2000 m. Note that in such configuration, every sensor in the second, third, and fourth coronas can reach at least two upstream coronas, for instance, the sensor in the third corona can even reach the sink directly. However, the sensor in the fifth corona and greater can reach only the next upstream corona, because of maximum transmission range limitation. In order to evaluate the performance of our proposal when the corona width is following an arithmetic progression, we suppose that according to the nominal communication range-based data forwarding, every sensor adopts a unique fixed transmission range to reach the subsequent upstream corona. However, according to our balanced routing solution, we assume that every sensor adopts at

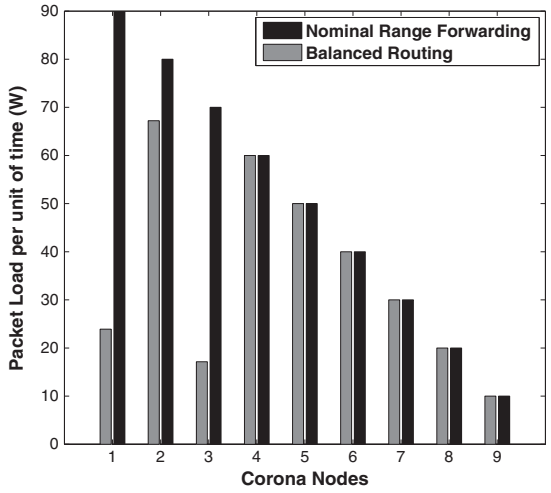

Figure 19. Packet load distribution per corona when $R = 2000\,\text{m}$, $r_0 = 50\,\text{m}$, $c_d = 50\,\text{m}$ and $d_{tx-max} = 400\,\text{m}$.

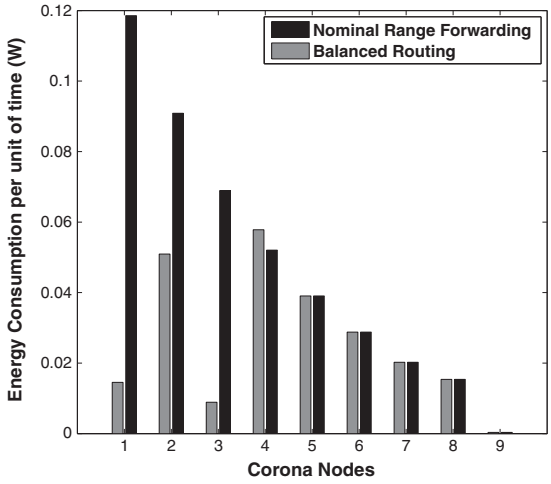

Figure 20. Energy consumption per corona when $R = 2000\,\text{m}$, $r_0 = 50\,\text{m}$, $c_d = 50\,\text{m}$ and $d_{tx-max} = 400\,\text{m}$.

maximum two possible transmission ranges to reach at most two subsequent upstream coronas whenever the 2-hop away corona is at a distance less that $d_{tx-\max} = 400\,\text{m}$. For instance, according to our study configuration, only the second, third, and fourth coronas can reach up to two subsequent upstream coronas; however, the transmission of all the remaining ones are limited only to the immediate subsequent corona. β^i vectors for each corona. Accordingly, in order to minimize the energy consumption gap between different coronas, sensors in coronas 2, 3, and 4 should send much more packets to the 2-hop away corona. The packet load distribution is shown in Figure 19.

Note that, the amount of accumulated traffic at coronas 4, 5, 6, 7, 8, and 9 is the same for both nominal communication range-based data forwarding and our balanced routing strategy as the transmission of their respective downstream coronas is limited to the 1-hop subsequent corona. However, coronas 1, 2, and 3 have less traffic that is why they are consuming less energy as shown in Figure 20.

Note that, although corona 4's accumulated traffic is the same for both routing strategy, the energy consumption of corona 4 according to our balanced routing strategy is more important than nominal range forwarding strategy as corona 4 has to send more traffic to the 2-hop away upstream corona, namely, corona 2, which is farther and thus necessitates more transmission energy. More importantly, it is worth noting that using our balanced routing strategy, leads to a maximum energy expenditure of 0.058 W at sensors in corona 4. However, according to the nominal communication range-based data forwarding, a maximum energy consumption of 0.118 W is achieved as expected at corona 1. Consequently, an energy saving of almost 51% is accomplished thanks to our balanced routing scheme even when the corona width is following an arithmetic progression. Consequently, we expect that even in temporally dynamic context our energy balanced scheme will achieve better results especially in terms of energy consumption.

6. CONCLUSIONS

In underwater environment, where solar energy cannot be exploited, operating on limited battery power imposes the use of energy efficient protocols. These protocols should be carefully designed in order to deal with the harsh characteristics of underwater communications such as high attenuation and bandwidth-limited channel. For these reasons, UW-ASNs require protocols that make judicious use of the limited battery budget while taking into account the unique features of the underwater channel. To this end, we proposed a dedicated deployment pattern along with the associated routing strategy that leads to an even energy depletion among all sensors in the network, and hence, the network lifespan is improved. Accordingly, by allowing each underwater node to dynamically adjust its transmission range among two possible levels, we determined for each source sensor the set of possible next hops with the associated transmission power and associated load weight that lead to a fair energy consumption, and hence, the energy sink hole problem is overcome. To do so, we developed a comprehensive analytical model that iteratively derives for each source sensor the appropriate load weight for each possible transmission range. Analytical results show that significant improvement is achieved by our routing scheme especially in terms of network lifetime compared with the nominal communication range-based data forwarding.

APPENDIX A

A.1. Proof of Equation (20)

In this paragraph, we provide a proof of Equation (20). Note that our goal is to calculate the cumulative traffic,

A_{j-k}, handled by a sensor in corona B_{j-k}, based on Equation (15).

Assume that $\forall 1 \leq j+1 \leq K$; $A_{j+1} = A$ and $\forall 0 \leq k \leq j-1$;

$$A_{j-k} = \left[\alpha_{0k} + \alpha_{1k}\beta_1^{j+1} + \alpha_{2k}\beta_2^{j+1}\right] \times A$$

where

$$\begin{aligned}
\beta_2^{j+1} &= 0; if k = j-1 \\
\alpha_{00} &= 1; \alpha_{0(-1)} = 1 \\
\alpha_{0k} &= 1 + \alpha_{0(k-1)}\beta_1^{j-(k-1)} + \alpha_{0(k-2)}\beta_2^{j-(k-2)} \\
\alpha_{1(-1)} &= 0; \alpha_{2(-1)} = 0; \alpha_{21} = 1; \alpha_{10} = 1; \alpha_{20} = 0; \\
\alpha_{1k} &= \alpha_{1(k-1)}\beta_1^{j-(k-1)} + \alpha_{1(k-2)}\beta_2^{j-(k-2)} \\
\alpha_{2k} &= \alpha_{2(k-1)}\beta_1^{j-(k-1)} + \alpha_{2(k-2)}\beta_2^{j-(k-2)}
\end{aligned}$$

If $k = 0; A_j = A + \beta_1^{j+1}A_{j+1} = A \times \left(1 + \beta_1^{j+1}\right) \Longrightarrow$ $\alpha_{00} = 1, \alpha_{10} = 1$ and $\alpha_{20} = 1$

Now, let us find by recurrence

$$A_{j-(k+1)},\ \forall 0 < k \leq j-1$$

According to Equation (15), we have

$$A_{j-(k+1)} = A + \beta_1^{j-k}A_{j-k} + \beta_2^{j-k+1}A_{j-(k-1)}$$

After extending the equation, we acquire

$$\begin{aligned}
A_{j-(k+1)} &= A + \beta_1^{j-k}\left[\alpha_{0k} + \alpha_{1k}\beta_1^{j+1} + \alpha_{2k}\beta_2^{j+1}\right] \times A + .. \\
&\beta_2^{j-(k-1)}\left[\alpha_{0(k-1)} + \alpha_{1(k-1)}\beta_1^{j+1} + \alpha_{2(k-1)}\beta_2^{j+1}\right] \times A \\
&= A \times \left[\left(1 + \alpha_{0k}\beta_1^{j-k} + \alpha_{0(k-1)}\beta_2^{j-(k-1)}\right) + + \left(\alpha_{1k}\beta_1^{j-k}\right.\right. \\
&\left.\left. + \alpha_{1(k-1)}\beta_2^{j-(k-1)}\right)\beta_1^{j+1} \right. \\
&\left. + \left(\alpha_{2k}\beta_1^{j-k} + \alpha_{2(k-1)}\beta_2^{j-(k-1)}\right)\beta_2^{j+1}\right]
\end{aligned}$$

$$\Longrightarrow$$

$$\begin{aligned}
\alpha_{0(k+1)} &= \left(1 + \alpha_{0k}\beta_1^{j-k} + \alpha_{0(k-1)}\beta_2^{j-(k-1)}\right) \\
\alpha_{1(k+1)} &= \left(\alpha_{1k}\beta_1^{j-k} + \alpha_{1(k-1)}\beta_2^{j-(k-1)}\right) \\
\alpha_{2(k+1)} &= \left(\alpha_{2k}\beta_1^{j-k} + \alpha_{2(k-1)}\beta_2^{j-(k-1)}\right)
\end{aligned}$$

Thus, we succeed to express the cumulative traffic at each iteration $j+1$ as a function of β^{j+1}. Based on this formula, we can calculate the energy consumption in transmission and reception to determine iteratively β^{j+1}.

Detailed derivation of the equations of transmission and reception energy are provided next.

A.2. The derivation of Equation (22)

Our objective is to calculate the average transmission energy, E_{TX}^i, consumed by a sensor in corona B_i and wedge W. According to Equation (16), we have

$$E_{TX}^i = \left[A_i\beta_1^i E_{tx}^1 + A_i\beta_2^i E_{tx}^2\right]$$

if $i = 1$ then $\beta_2^i = 0$

$$\begin{aligned}
E_{TX}^i &= A_i\left[\beta_1^i E_{tx}^1 + \beta_2^i E_{tx}^2\right] \\
&= \left(\beta_1^i E_{tx}^1 + \beta_2^i E_{tx}^2\right) A_{j-(j-i)} \\
&= \left(\beta_1^i E_{tx}^1 + \beta_2^i E_{tx}^2\right) \\
&\quad \times \left[\alpha_{0(j-i)} + \alpha_{1(j-i)}\beta_1^{j+1} + \alpha_{2(j-i)}\beta_2^{j+1}\right] \times A \\
&= A\left(\beta_1^i E_{tx}^1 + \beta_2^i E_{tx}^2\right)\alpha_{0(j-i)} + \\
&\quad + \sum_{l=1}^{2} A\left(\beta_1^i E_{tx}^1 + \beta_2^i E_{tx}^2\right)\alpha_{l(j-i)}\beta_l^{j+1} \\
&= TX_0^i + \sum_{l=1}^{2} TX_l^{j-i}\beta_l^{j+1}
\end{aligned}$$

if $j+1 = 1$ then $\beta_2^{j+1} = 0$

A.3. The derivation of Equation (23)

Now, let us derive the average reception energy, E_{RX}^i, consumed by a sensor in corona B_i and wedge W.

$$\begin{aligned}
&\forall\ 1 \leq j+1 \leq K \\
E_{RX}^{j+1} &= 0 \\
E_{RX}^{j} &= A\beta_1^{j+1}E_{rx}^1
\end{aligned}$$

Let us find $E_{RX}^i; \forall\ 1 \leq i < j+1$

$$E_{RX}^i = \beta_1^{i+1}A_{i+1}E_{rx}^1 + \beta_2^{i+2}A_{i+2}E_{rx}^2$$

if $i = j$ then $\beta_2^{i+2} = 0$

$$\begin{aligned}
E_{RX}^i &= A\beta_1^{i+1}E_{rx}^1\left[\alpha_{0(j-i-1)} + \alpha_{1(j-i-1)}\beta_1^{j+1} + \alpha_{2(j-i-1)}\beta_2^{j+1}\right] + ... \\
&\quad + A\beta_2^{i+2}E_{rx}^2\left[\alpha_{0(j-i-2)} + \alpha_{1(j-i-2)}\beta_1^{j+1} + \alpha_{2(j-i-2)}\beta_2^{j+1}\right] \\
E_{RX}^i &= A\left[\beta_1^{i+1}E_{rx}^1\alpha_{0(j-i-1)} + \beta_2^{i+2}E_{rx}^2\alpha_{0(j-i-2)}\right] + \\
&\quad + A\beta_1^{j+1}\left[\beta_1^{i+1}E_{rx}^1\alpha_{1(j-i-1)} + \beta_2^{i+2}E_{rx}^2\alpha_{1(j-i-2)}\right] + \\
&\quad + A\beta_2^{j+1}\left[\beta_1^{i+1}E_{rx}^1\alpha_{2(j-i-1)} + \beta_2^{i+2}E_{rx}^2\alpha_{2(j-i-2)}\right] \\
&= RX_0^i + RX_1^{j-i}\beta_1^{j+1} + RX_2^{j-i}\beta_2^{j+1}
\end{aligned}$$

If $i = j-1$ then $E_{RX}^i = RX_0^i + RX_1^{j-i}\beta_1^{j+1} + AE_{rx}^2\beta_2^{j+1}$

REFERENCES

1. Akyildiz IF, Pompili D, Melodia T. "Underwater acoustic sensor networks: research challenges". *Ad Hoc Networks (Elsevier)* 2005; **3**(3): 257–279.
2. Li J, Mohapatra P. Analytical modeling and mitigation techniques for the energy hole problem in sensor networks. *Pervasive and Mobile Computing (Elsevier)* 2007; **3**: 233–254.
3. Ammari H. Investigating the energy sink-hole problem in connected k-covered wireless sensor networks. *IEEE Transactions on Computers* 2013; **99**: 1–14.
4. Chen Y, Li Q, Fei L. Mitigating Energy Holes in Wireless Sensor Networks Using Cooperative Communication. In *IEEE 23rd International Symposium on Personal, Indoor and Mobile Radio Communications*, Sydney, NSW, 2012; 857–862.
5. Jiang F, Huang D, Yang C, Wang K. Mitigation Techniques for the Energy Hole Problem in Sensor Networks Using N-policy M/G/1 Queuing Models. In *International Conference on Theory Technologies and Applications, Frontier Computing*, Taiwan, Taichung, 2010; 281–286.
6. Wu X, Chen G, Das SK. Avoiding energy holes in wireless sensor networks with nonuniform node distribution. *IEEE Transactions on Parallel and Distributed Systems* 2008; **19**: 710–720.
7. Habib MA, Sajal KD. Promoting heterogeneity, mobility, and energy-aware Voronoi diagram in wireless sensor networks. *IEEE Transactions on Parallel AND Distributed Systems* 2008; **7**: 995–1008.
8. Pompili D, Akyildiz IF. Overview of networking protocols for underwater wireless communications. *IEEE Communications Magazine* 2009; **47**(1): 97–102.
9. Zorzi M, Casari P, Baldo N, Harris A. Energy-efficient routing schemes for underwater acoustic networks. *IEEE Journal on Selected Areas in Communications* 2008; **26**(9): 1754–1766.
10. Pompili D, Melodia T, Akyildiz IF. Routing algorithms for delay-insensitive and delay-sensitive applications in underwater sensor networks. In *Proceedings 12th ACM Annual International Conference Mobile Computer Network*, 2006; 298–309.
11. Jornet JM, Stojanovic M, Zorzi M. Focused beam routing protocol for underwater acoustic networks. In *Proceedings 3rd ACM International Workshop Underwater Network*, 2008; 75–82.
12. Zhou Z, Cui JH. Energy efficient multi-path communication for time-critical applications in underwater sensor networks, 2008; 221–230.
13. Pompili D, Akyildiz IF. A cross-layer communication solution for multimedia applications in underwater acoustic sensor networks. In *Proceedings 5th IEEE In. Conference Mobile Ad Hoc Sens. System*, 2008; 275–284.
14. Guo W, Liu Z, Wu G. An Energy-balanced transmission scheme for sensor networks, poster. *Proceedings First ACM International Conference Embedded Networked Sensor Systems (SenSys '03)* 2003: 300–301.
15. Bouabdallah F, Bouabdallah N, Boutaba R. On balancing energy consumption in wireless sensor networks. *IEEE Transactions on Vehicular Technology* 2009; **58**(6): 2909–2924.
16. Leone P, Nikoletseas S, Rolim J. An adaptive blind algorithm for energy balanced data propagation in wireless networks. In *Proceedings First IEEE International Conference Distributed Computing in Sensor Systems (DCOSS '05)*, 2005; 35–48.
17. Olariu S, Stojmenovic I. Design guidelines for maximizing lifetime and avoiding energy holes in sensor networks with uniform distribution and uniform reporting. *Proceedings IEEE INFOCOM '06* 2006: 1–12.
18. Lian J, Naik K, Agnew G. Data capacity improvement of wireless sensor networks using non-uniform sensor distribution. *International Journal Distributed Sensor Networks* 2006; **2**(2): 121–145.
19. Boukerche A, Chatzigiannakis I, Nikoletseas S. A new energy efficient and fault-tolerant protocol for data propagation in smart dust networks using varying transmission range. *Computer Communications* 2006; **4**(29): 477–489.
20. Brekhovskikh LM, Lysanov YP. *Fundamentals of Ocean Acoustics*. Springer-Verlag: New York, 1991.
21. Stojanovic M. On the relationship between capacity and distance in an underwater acoustic communication channel, ACM SIGMOBILE Mobile Comput. *Communications Review* 2007; **11**(4): 34–43.
22. Jornet JM, Stojanovic M, Zorzi M. On joint frequency and power allocation in a cross-layer protocol for underwater acoustic networks. *IEEE Journal Of Oceanic Engineering* 2010; **35**(4): 936–947.
23. Powell O, Leone P, Rolim J. Energy optimal data propagation in wireless sensor networks. *Journal Parallel and Distributed Computing* 2007; **3**(67): 302–317.
24. Wu X, Chen G, Das SK. On the energy hole problem of nonuniform node distribution in wireless sensor networks, third. In *Proceedings IEEE International Conference Mobile Ad-Hoc and Sensor Systems (MASS '06)*, 2006; 180–187.

AUTHORS' BIOGRAPHIES

Chaima Zidi received his Computer Science Engineering and Masters degrees from the National College of Computer Science (ENSI, Tunisia) in 2010 and 2011, respectively. At the beginning of 2013, she joined the Faculty of Computing and Information Technology (Jeddah, Saudi Arabia). Now, she prepares a Ph.D in Underwater Acoustic Sensor Networks within LIPADE Laboratory (Paris, France).

Fatma Bouabdallah received a B.S. degree in computer engineering from Ecole Nationale des Sciences de l'Informatique (ENSI), Tunis, Tunisia, in 2005, and the M.S. degree in network and computer science from the University of Paris VI, France, in 2006. She attended the doctoral program at the Institut National de Recherche en Informatique et en Automatique, Rennes, France from October 2006 to November 2008. In November 2008, she received her Ph.D. degree in computer science. In 2010, she was with the University of Waterloo, Canada, as a Postdoctoral Fellow. She is currently an assistant professor in King AbdulAziz University, Jeddah, Saudi Arabia. Her research interests include wireless sensor networks, underwater acoustic sensor networks, cross-layer design, and modeling and performance evaluation of computer networks.

Raouf Boutaba received the M.Sc. and Ph.D. degrees in computer science from the University Pierre Marie Curie, Paris, in 1990 and 1994, respectively. He is currently a professor of computer science at the University of Waterloo. His research interests include resource and service management in networks and distributed systems. He is the founding editor in chief of the IEEE Transactions on Network and Service Management (2007–2010) and on the editorial boards of other journals. He has received several best paper awards and other recognitions such as the Premiers Research Excellence Award, the IEEE Hal Sobol, Fred W. Ellersick, Joe LociCero, Dan Stokesbury, Salah Aidarous Awards, and the McNaughton Gold Medal. He is a fellow of the IEEE, the Engineering Institute of Canada, and the Canadian Academy of Engineering.